JOURNAL OF MATERIALS SCIENCE 37 (2002) 3835–3839

In Situ observations of the evolution of precipitates on the surface of Al-6022

L. C. BRABIE, S. SRIDHAR
Department of Materials Science and Engineering, Carnegie Mellon University, Pittsburgh, PA 15213, USA
E-mail: sridhars@andrew.cmu.edu

The precipitation of Mg_2Si on the surface of Al 6022 has been investigated *in situ* using a Confocal Scanning Laser Microscope and a gold image furnace during cooling and isothermal conditions. It was found that precipitates form during cooling at temperatures between 400 and 280°C. The numbers and size of precipitates, as well as the growth velocity have been obtained as function of temperature for different cooling rates. The growth of precipitates has been modeled by means of a normalized Gaussian function, which can be used to predict the precipitate evolution.

1. Introduction

Al-Mg-Si alloys (the 6XXX series) are an important group of medium-strength structural alloys that are used in the automotive and shipbuilding industries. In general, the 6XXX series exhibit good weldability and corrosion resistance [1] together with strength obtained from the precipitation of metastable precursor. Due to the industrial need to optimize the structure of cast ingots before extrusion the problem of high-temperature precipitation and growth in Al-Mg-Si alloy is of great importance. The understanding and control of precipitation is critical for achieving the optimal properties, and therefore several studies have been conducted on how the structure changes after cooling and high temperature annealing [2–7].

Miao and Laughlin [2, 3] reported for a supersaturated solid solution of Al-0.55wt%Mg-1.28wt% Si-0.07 wt%Cu that the equilibrium precipitates obtained on heating (10°C/min) were β (Mg_2Si), Q ($Al_5Cu_2Mg_8Si_6$) and Si for temperatures below 300°C. In the temperature range of 300 and 540°C, the equilibrium precipitates were found to be β and Si.

In a recent study Edwards *et al.* [4] proposed the following precipitation sequence on heating (5°C/min) for an alloy of Al-0.8wt%Mg-0.79wt%Si-0.18wt%Cu: Clusters of Si and/or Mg atoms ⇒ Dissolution of Mg clusters ⇒ Formation of Mg/Si co-clusters ⇒ Small precipitates of unknown structure ⇒ β'' precipitates ⇒ B′ and β'' precipitates ⇒ β(Mg_2Si) precipitates

The authors also reported that the Mg : Si ratios in the B′ and β'' precipitate were close to 1.1.

Murayama *et al*. [5] studied the structure of precipitates in two alloys, Al-0.63%Mg-0.35%Si and Al-0.64%Mg-0.81%Si (excess of silicon). The Mg : Si atomic ratios of the β' and β phases were found to be 1.75 and 2.10, respectively, for the alloy with 0.35% Si and 1.21 and 2.13 in the one with excess silicon.

Matsuda *et al*. [6], using a EDS technique, reported a Mg : Si atomic ratio of the β' phase a value of 1.68 while Lynch *et al.* [7] determined by the same technique that the Mg : Si ratio is much less than 2 : 1, possibly as low as 0.44.

In this study the behavior of precipitates in the aluminium alloy 6022 has been investigated *in situ* by the use of the Confocal Scanning Laser Microscope in order to provide more information on the rates of precipitation, nucleation, growth and shape change at high temperatures.

The objectives of this paper are to observe the formation of precipitates and correlate the temperature and time with the growth rate of the precipitates at different cooling rates together with the phase analyses and precipitate identification. Furthermore, this study intends to provide experimentally based rate equations for precipitate evolution that can be readily incorporated into multi-scale models for prediction of microstructural evolution during thermal and thermo-mechanical processing of Al-6XXX series alloys.

2. Experimental technique

Samples of the commercial aluminium alloy 6022 were supplied by ALCOA Technical Center in the form of rolled sheet of 2 mm thick with the following composition: Al-1.15%Si-0.575%Mg-0.06% Cu-0.06%Mn-0.12%Fe. In the current study 6022 samples of 4 × 4 × 2 mm dimensions were placed inside a Al_2O_3 crucible which was inserted into the hot-stage. The hot stage consisted of a gold image furnace where the radiation from a halogen lamp was radiated and focused onto the sample with golden mirrors. Temperature control and measurements were achieved through a thermocouple attached near the wall of the crucible. The chamber was filled with purified Ar-gas and then evacuated by the use of a diffusion pump. This procedure was repeated three times. A Ti foil was wrapped around the Al_2O_3 crucible in order to remove any residual oxygen. Subsequently, the samples were heated under purified Ar atmosphere at a rate of 1°C/sec to 350,

400 and 550°C, maintained for 10 to 60 minutes and then cooled at various cooling rates in order to observe precipitation evolution during cooling. The following cooling rates were employed 1, 2, 3, 3.9 and 4.2°C/sec.

Laser confocal microscopy was used to visualize the precipitation at various temperatures. Confocal scanning laser microscopy (CSLM), equipped with a hot-stage, combines the advantages of confocal optics and a He-Ne laser and makes it thereby possible to observe samples at high resolution at elevated temperatures. The confocal optics enables the detection of a strong signal from the focal plane while decreasing the intensity of signals not in the focal plane. By scanning a surface at various focal depths, a 3D image is constructed and thus images of uneven samples with depths and pimples can be obtained. The utilization of laser results in high illumination intensity compared to the thermal radiation at elevated temperatures and thus increases the resolution between different phases. This technique is ideally suited for *in situ* study of chemical reactions and phase transformations at the surface of metals at elevated temperatures.

The obtained CSLM images were continuously captured with Charge Coupled Device (CCD) and recorded with a video recorder and frames of pertinent sequences were exported to a computer to be analyzed. The precipitate evolution was quantified by using a computer image analysis program, NIH 1.62 [8].

Scanning Electron Microscope (SEM), equipped with an Energy Dispersion X-ray Spectroscopy (EDS) unit was used to study the composition of the surface precipitates after cooling.

3. Results and discussions

The focus of this work was to obtain real-time kinetic data for the evolution of precipitates upon (i) cooling at 1, 2, 3, 3.9 and 4.2°C/sec after annealing for 10 minutes at 550°C and (ii) isothermal aging at 300 and 400°C. The precipitates formed were analyzed after each experiment through SEM-EDS. The EDS analysis of the samples after experiments shows the ratio of Mg/Si was mostly in the range of 1.13 to 1.25 and a few cases as Mg/Si = 2. The results obtained for the precipitate analyses are in good agreement with those obtained by Murayama *et al.* [5] and Edwards *et al*. [4].

3.1. Precipitation process on cooling

Fig. 1 shows the observed sequence of precipitate evolution at different temperatures during cooling for a typical experiment. The alloy was heated up to 550°C at a heating rate of 1°C/s, held 10 minutes, and then allowed to cool down to room temperature with a cooling rate of 4.2°C/s. The precipitates start to form in the temperature range 400–280°C. The precipitate shapes were approximated as ellipsis and the dimensions were characterized as the measured major and minor axis of the ellipsis. Therefore, the aspect ratios were evaluated as functions of time. Fig. 2 shows the change in precipitate's shape represented by the aspect ratio with time, for different cooling rates. The x-axis has been normalized such that, $t = 0$ s, corresponds to the

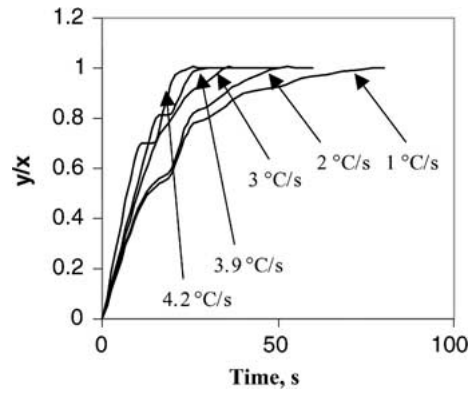

Figure 2 Shape change of the precipitates function of time.

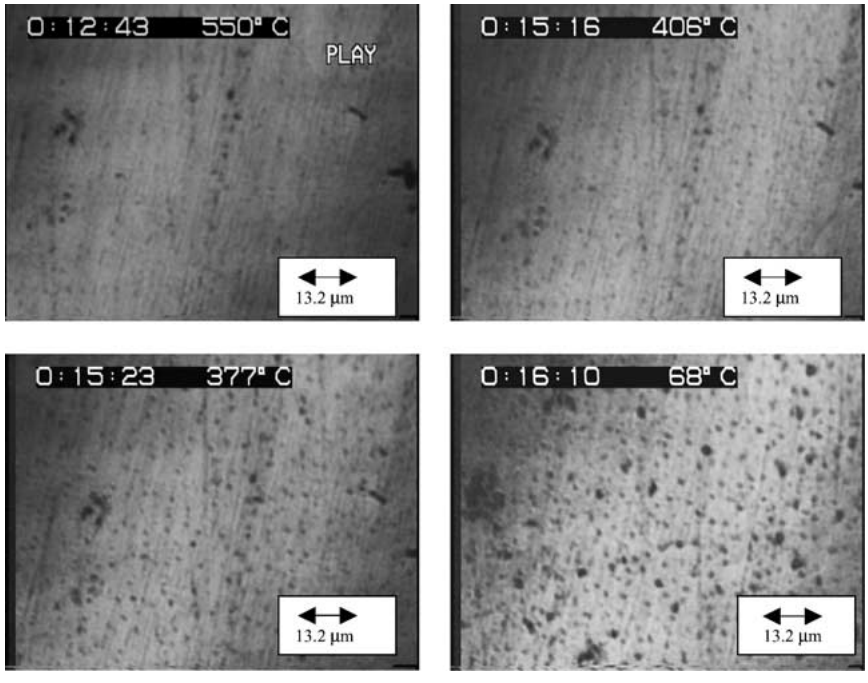

Figure 1 Precipitation sequence in a typical experiment.

TABLE I Experimental conditions and results: Cooling experiments

Experiment number	Temperature, T (°C)	Growth velocity of the precipitate, V (μm/s)	Cooling rate, R (°C/s)	Number of precipitates, $n_{\max}$ (μm^2)	T_N (°C)	T_σ (°C)
1	550	0.0022–0.005	4.2	0.078–0.1	163.4	20
2	550	0.0033–0.006	3.9	0.086–0.114	164	21
3	550	0.0034–0.0065	3	0.09–0.13	165	20
4	550	0.0035–0.0067	2	0.087–0.13	163.1	24
5	550	0.0036–0.00685	1	0.092–0.14	164	19

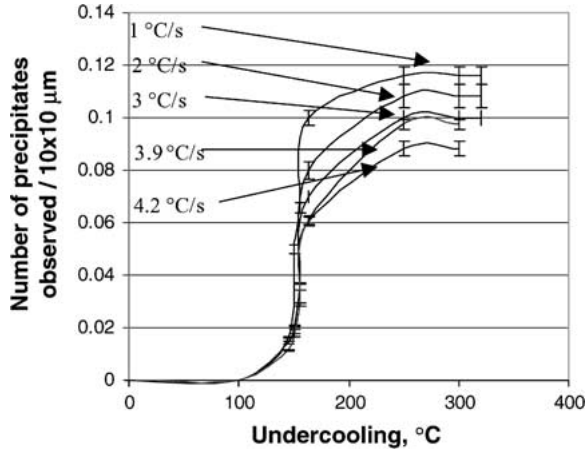

Figure 3 Number of precipitates formed as function of cooling rate.

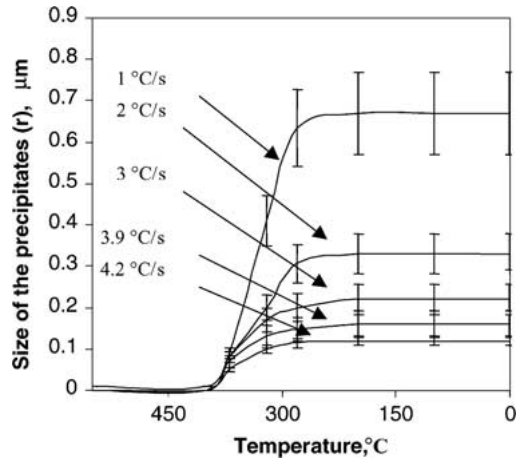

Figure 4 Size of the precipitates as a function of different cooling rates.

time when precipitates were first observed. It can be seen that in all cases the precipitates show an elongated shape, but eventually, the shape can be seen as circular form. Fig. 3 shows the increase in the number of precipitates during cooling for the different cooling rates. The scattering is shown with vertical bars. By decreasing the cooling rate from 4.2 to 1°C/s the number of precipitates formed increases from ∼8.5 up to ∼12 for an area of 10×10 μm. Below 280°C the formation of new precipitates was not observed.

Assuming that the precipitates are growing uniform with a circular shape, the statistical growth velocity of the radius (r) was in the range of 0.0022 to 0.0051 μm/s for a cooling rate of 4.2°C/s. By decreasing the cooling rate to 1°C/s, an increase in the growth rate up to 0.00685 μm/s was observed, as it can be seen in Table I. Fig. 4 shows the growth of precipitates function of different cooling rates from 550°C. The vertical bars show the scatter in the experimental data. The scatter is primarily due to the uncertainties in determining the precipitate sizes during image analysis cause by e.g., shadows. As it can be seen the final precipitate size is in the range of 0.2 to 1 μm diameter.

In the case of the samples heated up to 400°C and then cooled down at various cooling rates, the results show that the number of precipitates formed is much less than for samples cooled from 550°C. As a comparison between samples cooled down from 400 and 550°C with same cooling rate of 3°C/s the number of precipitates detected are 5 and 13, respectively, for an area of 10×10 μm. The small number of precipitates visualized in the case of sample cooled from 400°C in comparison to that from 550°C is due to the fact that the solvus temperature for equilibrium precipitates should be approximately ∼400°C. Precipitates smaller than 0.1 μm in diameter could not be detected with CLSM, and thus a more precise thermodynamic comparison is not possible.

For the samples heated up to 350°C and then cooled down to room temperature the results obtained are uncertain since the particles are too small to be analyzed.

3.2. Precipitation rate equations

An approach of Charbon and Rappaz [9] to describe the grain nucleation during solidification was employed in order to obtain the function governing the process of precipitates formed during cooling. This model assumes that the, number of precipitates that are formed ($\mathrm{d}n_p$), during an incremental temperature step ($\mathrm{d}T$) can be obtained from the following relationship:

$$\frac{\mathrm{d}n_p}{\mathrm{d}T} = \frac{n_{\max}}{T_\sigma\sqrt{2\pi}} \exp\left(-\frac{(T - T_N)^2}{2T_\sigma^2}\right) \qquad (1)$$

where n_{max} is the maximum number of precipitates, taken as average value of the number of precipitates from several areas, T_σ and T_N are the deviation and the mean respectively of a normalized Gaussian temperature distribution function. Physically, the model can be viewed as a total number of $n_{\max}$ nucleation sites existing, but possessing different potentials for heterogeneous nucleation characterized by $\mathrm{d}n_p/\mathrm{d}T$ vs. T. The initial rise in the Gaussian distribution could thus be interpreted as more nuclei being activated as the undercooling is increased. The decay of the Gaussian distribution can be viewed as being caused by the decreasing amount of un-activated nucleation sites. The parameters in Equation 1 are expected to vary with cooling rate and Fig. 5 shows the observed cooling rate dependence of the three parameters for the precipitation formation and

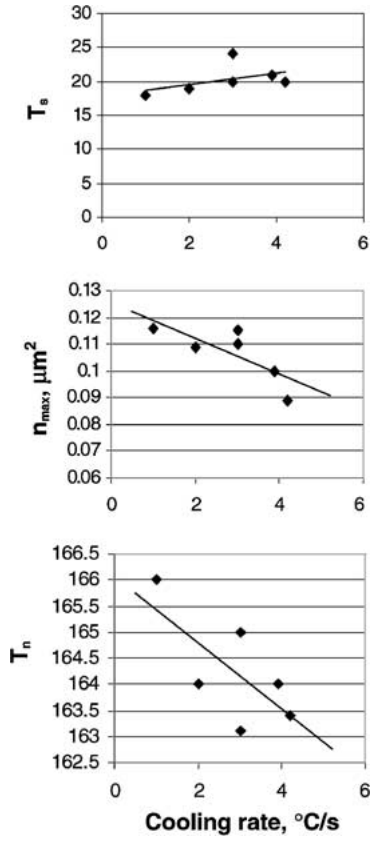

Figure 5 Parameters dependence on cooling rate as shown in Equations 2–4, respectively.

the numerical parameters derived by a least squares fitting are given below:

$$n_{\max} = -0.0067R + 0.1256 \quad (2)$$

$$T_N = -0.6318R + 166.05 \quad (3)$$

$$T_\sigma = 0.8714R + 17.85 \quad (4)$$

where the range of applicability is $4.2 < R < 1$°C/s. The relations have been evaluated by determining the average $n_{\max}$, T_σ and T_N for 20 particles at each cooling rate. While the linear fits were far from ideal (Fig. 5) it should be mentioned that Equations 2–4 are intended only as empirical corrections to account for the effect of cooling rate in Equation 1. It is difficult at this stage to relate the observations to classical nucleation theory since nucleation is likely occurring at a range of sites with various nucleation potentials.

Fig. 6 shows the Gaussian distribution (thin line) fitted to the number of precipitates during a typical experiment and compared to a Gaussian distribution predicted by the model. The mismatch in Fig. 6 is mainly due to the sudden increase in the number of precipitates at around 400°C. The curves are representative for the observed precipitation formation on the surface of the material. The number of precipitates increases as function of decreasing the cooling rate. At low temperatures (<280°C) the number and size of the precipitates formed are too small to be visualized by the CSLM. Equation 1 in combination with the empirical relations from Equations 2 to 4 can be used to predict the precipitate evolution, e.g. Finite Element simulations of thermochemical processes of Al-6XXX series alloy.

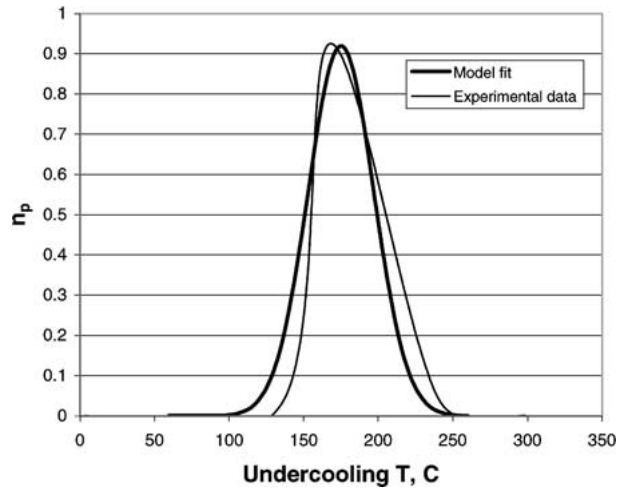

Figure 6 Comparison between the Gaussian distribution predicted by the model to the experimental data.

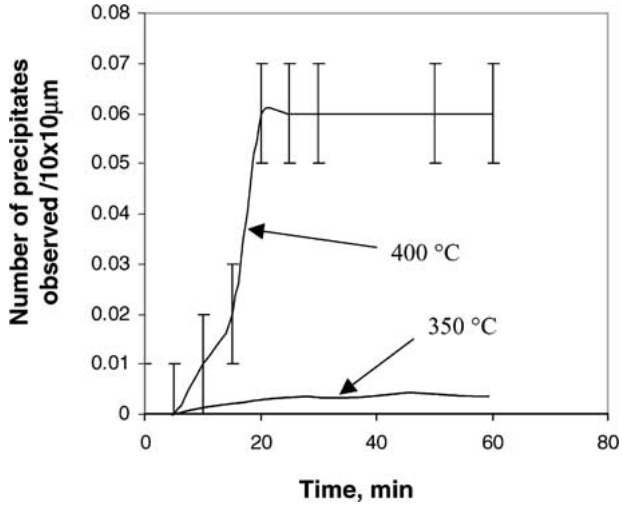

Figure 7 Number of precipitates formed as function of time, for samples held at 400 and 350°C for 60 minutes.

3.3. Isothermal precipitation process

Isothermal annealing experiments were conducted by rapidly cooling the samples, after heat treatment at 550°C, to the desired temperatures and maintaining a constant temperature for 60 minutes. The precipitate evolution 350 and 400°C were studied in this way.

Fig. 7 shows the number of precipitates observed during the two temperatures. While at 350°C the precipitates were too small to be quantify the process accurately through the CLSM, it can be seen at 400°C that there is a sudden increase between 5–20 minutes after which the process seems to be complete. Fig. 8 shows the increase in the precipitate size during annealing at 400°C. The size change, characterized by changes in radius r, of a circle, with equivalent area as the precipitate was found to be same for all particles regardless of shape. Fig. 8 shows the average results for 32 precipitates. Fig. 9 shows the change in aspect ratio y/x, for two types of precipitates, during the isothermal treatment at 400°C. Results show that the precipitates become either circular or elongated. The shapes discussed here are the 2D morphologies observed on the surface. The ratio between circular and elongated type precipitates was 2. SEM-EDS analysis did not detect any consistent composition differences between the

TABLE II Experimental conditions and results: Isothermal experiments

Experiment	Annealing temperature, T (°C)	Time (min)	Growth velocity of the round shape precipitate, V (μm/s)	Growth velocity of the lath type shape precipitate, V_x, V_y (μm/s)	Number of precipitates, n_{max} (μm^2)
1	550	60	0.00055–0.0008	$V_y = 0.00041$ $V_x = 0.00016$	0.05–0.07
2	400	60	0.00051–0.00079	$V_y = 0.00038$ $V_x = 0.00017$	0.04–0.06

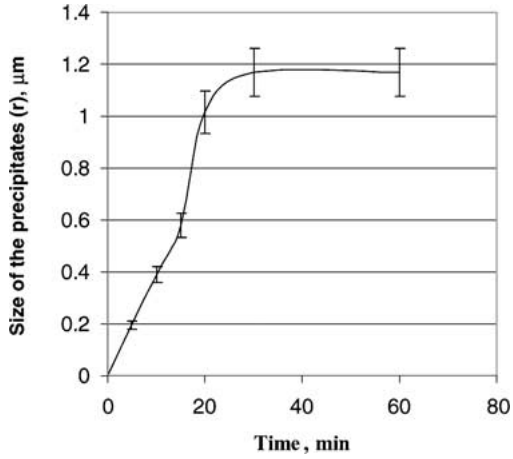

Figure 8 Growth of the precipitates for isothermal experiments at 400°C for 60 minutes.

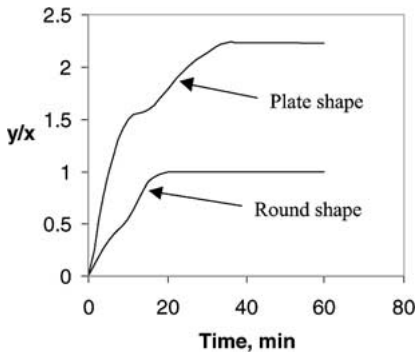

Figure 9 Shape change of the precipitates function of time during annealing at 400°C for 60 minutes.

circular and elongated shape precipitates. Table II summarizes the experimental results obtained.

4. Conclusions

The evolution of Mg_xSi_y precipitates on the surface of Al-6022 samples was investigated through *in situ* observations using a Confocal Laser Electron Microscope. During cooling after annealing at 550°C it was observed that:

- the precipitation process started at 400°C and ends at 280°C and in this range the precipitation can be expressed by a normalized Gaussian distribution suggesting that the nucleation process during cooling which can be explained as a heterogeneous process were a set amount of nucleation sites of various potentials are activated.
- the precipitates change in shape from needle like shape to circular.

During isothermal treatment it was observed that:

- when annealing at 400°C, there is a sudden increase in the number of precipitates formed until 20 minutes after which the precipitate density remained constant. The steep step-like nucleation vs. time behavior further suggests a heterogeneous nucleation event were nucleation sites with a narrow range of nucleation potentials are active.
- the precipitate shape changed during the treatment and resulted in either circular or elongated precipitates.

References

1. G. B. BURGER, A. K. GUPTA, P. W. JEFFREY and D. J. LLOYD, *Mater. Charact* **35** (1995) 23.
2. W. F. MIAO and D. E. LAUGHLIN, *Met. and Mat. Trans.* A **31A** (2000) 361.
3. *Idem.*, *Scripta Mater.* **40**(7) (1999) 873.
4. G. A. EDWARDS, K. STILLER, G. L. DUNLOP and M. J. COUPER, *Acta Mater.* **46**(11) (1998) 3893.
5. M. MURAYAMA and K. HONO, *ibid.* **47**(5) (1999) 1537.
6. K. MATSUDA, Y. SAKAGUCHI, Y. MIYATA, Y. UETANI, T. SATO, A. KAMIO and S. IKENO, *J. Mater. Sci.* **35** (2000) 179.
7. J. P. LYNCH, L. M. BROWN and M. H. COOPER, *Acta Metall.* **30** (1982) 1389.
8. Public domain image processing and analysis program for the Macintosh developed at the *Research Services Branch (RSB)* of the National Institute of Mental Health (NIMH).
9. C. CHARBON and M. RAPPAZ, *Mod. Sim. Mater. Sci. Eng.* **1** (1993) 455.

Received 5 December 2001
and accepted 17 May 2002